Research Article

Molecular Structure, Spectroscopic Investigation, DFT Calculations and Other Biomolecular Properties of 1,2,3-trichloro-4-nitrobenzene

S. Jeyavijayan[1],* S. Manimaran[2], I. Vigneshwari[1], B. Vijitha[1]
1. Department of Physics, Kalasalingam University, Krishnankoil, Tamilnadu-626 126, India.
2. P.G.&Research Department of Physics,Thanthai Hans Rover College, Perambalur, India.
***Corresponding author's E-mail:** sjeyavijayan@gmail.com

Received: 08-01-2018; **Revised:** 02-02-2018; **Accepted:** 11-02-2018.

ABSTRACT

The experimental FTIR (4000–400 cm-1) and FT-Raman spectra (3500-50 cm-1) of 1,2,3-trichloro-4-nitrobenzene (TCNB) in solid phase have been recorded. The density functional theoretical (DFT) computations were performed at the B3LYP quantum chemical method with 6-31+G(d,p) and 6-311++G(d,p) basis sets to derive the optimized geometric parameters and vibrational frequencies. The theoretical vibrational spectral characteristics of TCNB are compared with the experimental results. The assignments of the vibrational frequencies have been confirmed by total energy distribution (TED) analysis. The possible electronic transitions are determined by HOMO–LUMO orbital shapes and their energies using the same theoretical calculations. TCNB exhibited good nonlinear optical activity and was much greater than that of urea. The charge density distribution and site of chemical reactivity of the molecule have been obtained by molecular electrostatic potential (MESP) studies. In addition, natural bond orbital (NBO), Mulliken charges and thermodynamic properties were also investigated.

Keywords: FTIR; FT-Raman; DFT calculations; 1,2,3-trichloro-4-nitrobenzene ; NBO.

INTRODUCTION

Benzene derivatives have been widely used to manufacture therapeutic chemicals, dyes, artificial leather and detergent products. The substituted benzene derivatives with high optical non-linearities are very promising materials for future optoelectronic and non-linear optical applications. Particularly, the new non-linear optical crystal of chloro and nitro substituted benzene has been grown by low temperature solution growth technique. The optical transparency of this crystal is quite good and hence it can be a potential material for frequency doubling of non-linear optics[1]. When substituted benzene molecules undergo electrophilic substitution reactions, substituents on a benzene ring can influence the reactivity. Most of the nitrobenzene is consumed in the production of aniline which is used as starting materials in a vast amount of chemicals, pharmaceuticals, dyes, electro-optical and many other industrial processes[2]. The inclusion of substituents in benzene leads to the variation of charge distribution in the molecule, and consequently affects the structural, electronic and vibrational parameters. Because of these versatile behaviors of benzene, Mahadevan *et al.*[3], have extensively reported the FTIR and FT-Raman, UV spectroscopic investigation of 1-bromo-3-fluorobenzene using DFT calculations. Further, the molecular structure and conformation of 1, 3, 5-tris (trifluoromethyl)benzene by gas-phase electron diffraction and quantum chemical calculations have been investigated by Kolesnikova *et al.*[4]. The spectroscopic study of human hemoglobin structural and functional alterations and heme degradation upon interaction with benzene was studied by Hosseinzadeh *et al.*[5]. More recently, Vennila *et al.*[6] investigated a complete computational and spectroscopic study of 2-bromo-1,4-dichlorobenzene. Literature survey reveals that, no density functional theory (DFT) with 6-31G+ (d, p) and 6-311++G(d,p) basis set calculations of 1,2,3-trichloro-4-nitrobenzene (TCNB) have been reported so far. Therefore, an attempt has been made in the present investigation to study the detailed theoretical (DFT) and experimental (FTIR and FT-Raman) investigation of the vibrational spectra of TCNB.

MATERIALS AND METHODS

The compound TCNB was purchased from Lancaster Chemical Company, UK which is of spectroscopic grade and hence used for recording the spectra as such without any further purification. The FTIR spectrum of the compound was recorded in the range of 4000-400 cm^{-1} using a BRUKER IFS-66V FTIR spectrometer equipped with an MCT detector, a KBr beam splitter and a globar source. The spectral resolution is $\pm$ 1 cm^{-1}. The FT-Raman spectrum of TCNB has been recorded in the Stokes region (3500-50 cm^{-1}) on a computer interfaced BRUKER IFS model interferometer equipped with FRA-106 FT-Raman accessory using Nd:YAG laser source operating at 1.064 nm excitation wavelengths, line widths with 200 mW power. The frequencies of all sharp bands are accurate to $\pm$ 1 cm^{-1}.

Computational Details

DFT calculations were reported to provide excellent vibrational frequencies of organic molecules if the calculated frequencies are scaled to compensate for the approximate treatment of electron correlations, for basis set deficiencies, and for anharmonicity. A number of

studies have been carried out regarding the calculations of vibrational spectra using B3LYP method with the 6-31+G (d,p) and 6-311++G(d, p) basis sets. As a result, it was found that the experimental vibrational frequencies and IR intensities could be reported very accurately. In this study, all calculations were performed using the Becke-3-parameter hybrid functional (B3) for exchange part and the Lee-Yang-Parr (LYP) correlation function[7, 8], with 6-31+G(d, p) and 6-311++G(d, p) as the basis sets using the GAUSSIAN 09W suite of program[9]. The basis sets 6-31+G(d,p) and 6-311++G(d, p) are a triple-split valance basis sets that increases the flexibility of the valence electrons. All the parameters were allowed to relax and all the calculations converged to an optimized geometry which corresponds to a true minimum, as revealed by the lack of imaginary values in the wavenumber calculations. The Cartesian representation of the theoretical force constants have been computed at the fully optimized geometry. Transformation of force field and calculation of the total energy distribution (TED) were done on a PC with the MOLVIB program (version V7.0-G77) written by Sundius[10]. To understand the clear evidence of stabilization originating from the hyper conjugation of various intermolecular interactions, natural bond orbital analysis with B3LYP/6-311++G(d,p) method have been calculated. The HOMO and LUMO analyses have been used to elucidate information regarding charge transfer and chemical reactivity of the molecule.

RESULTS AND DISCUSSION

Molecular geometry

The optimized molecular structure of TCNB is shown in Fig. 1. The most optimized structural parameters calculated by DFT/B3LYP with 6-31+G(d,p) and 6-311++G(d,p) basis sets are compared with X-ray diffraction experimental data[11,12] and represented in Table 1. From the theoretical values, it is found that most of the optimized bond lengths are slightly larger than the experimental values, due to that the theoretical calculations belong to isolated molecule in gaseous phase while the experimental results belong to molecule in solid state. The calculated geometrical parameters represent a good approximation and they are the bases for calculating other parameters, such as vibrational frequencies and thermodynamics properties.

Table 1: Optimized geometrical parameters of 1, 2, 3-trichloro-4-nitrobenzene obtained by B3LYP/6-31+G(d, p) and 6-311++G(d, p) basis sets.

Parameters	Method/Basis set		Experimental[a]
	B3LYP/ 6-31+G(d,p)	B3LYP/ 6-311++G(d,p)	
Bond length (Å)			
C1-C2	1.404	1.401	1.396
C1-C6	1.395	1.391	1.387
C1-Cl7	1.738	1.738	1.721
C2-C3	1.415	1.411	1.396
C2-Cl8	1.735	1.735	1.721
C3-C4	1.411	1.407	1.387
C3-Cl9	1.730	1.730	1.721
C4-C5	1.397	1.393	1.388
C4-N10	1.485	1.492	1.471
C5-C6	1.384	1.380	1.388
C5-H13	1.081	1.080	1.087
C6-H14	1.083	1.081	1.081
N10-O11	1.225	1.218	1.225
N10-O12	1.233	1.225	1.228
Bond angle (^{0})			
C2-C1-C6	120.50	120.55	121.0
C2-C1-Cl7	121.21	121.21	120.7
C6-C1-Cl7	118.28	118.23	118.9
C1-C2-C3	120.14	120.10	118.6
C1-C2-Cl8	119.59	119.57	118.9
C3-C2-Cl8	120.26	120.31	120.2
C2-C3-C4	118.26	118.28	118.6

C2-C3-Cl9	117.85	117.88	118.9
C4-C3-Cl9	123.88	123.82	120.7
C3-C4-C5	120.69	120.65	119.4
C3-C4-N10	124.02	124.09	121.3
C5-C4-N10	115.28	115.24	119.3
C4-C5-C6	120.68	120.71	120.6
C4-C5-H13	118.35	118.31	119.3
C6-C5-H13	120.95	120.96	121.3
C1-C6-C5	119.71	119.67	119.3
C1-C6-H14	119.64	119.65	119.7
C5-C6-H14	120.63	120.66	121.3
C4-N10-O11	119.32	119.18	118.3
C4-N10-O12	116.51	116.38	119.1
O11-N10-O12	124.16	124.43	123.5

[a]Experimental values are taken Ref. [11, 12]

The optimized molecular structure of TCNB reveals that the para-substituted nitro group and chlorine atoms at first, second and third positions are in planar with the benzene ring. Inclusion of nitro group and chlorine atoms known for their strong electron-withdrawing nature is expected to increase a contribution of the resonance structure, in which the electronic charge is concentrated at this site. This is the reason for the increase in bond lengths of C1-Cl7 (1.738 Å), C2-Cl8 (1.735 Å) and C3-Cl9 (1.730 Å). The carbon atoms are bonded to the hydrogen atoms with an σ-bond in benzene and the substitution of nitro group and chlorine atoms for hydrogen reduces the electron density at the ring carbon atom. The ring carbon atoms in substituted benzenes exerts a larger attraction on the valence electron cloud of the hydrogen atom resulting an increase in the C-H force constants and a decrease in the corresponding bond length (~1.08 Å). The benzene ring appears to be a little distorted because of the halogen atoms as seen from the bond angles calculated. For chlorine atoms at first, second and third positions of the benzene ring, the bond angles C2–C1–C6, C1–C2–C3 and C2–C3–C4 are calculated as 120.5°, 120.14° and 118.26°, respectively. The bond angle C3–C4–C5 for nitro group at fourth position is calculated as 120.6°. They are differing from the typical hexagonal angle of 120°. These asymmetries of the exocyclic angles reveal the repulsion between chlorine atoms, nitro group and the benzene ring.

Vibrational spectra

The TCNB consists of 14 atoms, hence undergoes 36 normal modes of vibrations. In agreement with C_s symmetry, the 36 fundamentals are distributed amongst the symmetry species as

$$\Gamma_{3N-6} = 25\ A'\ (\text{in-plane}) + 11\ A''\ (\text{out-of-plane})$$

The observed FTIR and FT-Raman spectra of TCNB are shown in Fig. 2. The detailed vibrational assignment of fundamental modes of TCNB along with the calculated IR and Raman intensities and normal mode descriptions (characterised by TED) are reported in Table 2.

The reliable prediction of vibrational spectra is of considerable use in assigning the normal modes of a molecule. Computational methods can also be used to assign the bands of the spectra. The selection of adequate quantum chemical methods and scaling procedures remarkably reduces the risk in the assignment and can accurately determine the contribution of the different modes in an observed band. DFT calculations were reported to provide excellent vibrational frequencies of organic molecules if the calculated frequencies are scaled to compensate for the approximate treatment of electron correlations, for basis set deficiencies, and for anharmonicity. However, the introduction of scaling factors is capable of accounting for all these effects. In this study, a better agreement between the computed and experimental frequencies can be obtained by using scale factor[13] of 0.96 for B3LYP method. The resultant scaled frequencies are also listed in Table 2.

C-H vibrations

In the experimental spectrum, C–H stretching frequencies appear in the range 3100-3000 cm^{-1}, the C–H in-plane bending vibrations[14] in the range 1300-1000 cm^{-1} and C–H out-of-plane bending vibrations in the range 1000-750 cm^{-1}. In the present study, the FTIR vibrational frequencies at 3155 and 3120 cm^{-1} are assigned to C–H stretching vibrations of TCNB and show good agreement with the calculated results. The Raman counterparts of C-H vibrations are observed at 3150 and 3118 cm^{-1}, which are further supported by the TED contribution of almost 100%. The IR band at 1190 cm^{-1} and Raman band at 1182 cm^{-1} are assigned to C–H in-plane vibrations of TCNB. The C–H out-of-plane bending vibrations of the molecule are found at 780 cm^{-1} in IR and 795 cm^{-1} in the Raman spectrum. These modes show consistent agreement with the computed B3LYP results.

C-C vibrations

The C-C aromatic stretching vibrations[15] gives rise to characteristic bands in both the observed IR and Raman spectra, covering the spectral range from 1650 to 1400 cm^{-1}. Therefore, the C-C stretching vibrations of TCNB are found at 1520, 1422, 1390 cm^{-1} in FTIR and 1525, 1494, 1450, 1435 cm^{-1} in the FT-Raman spectrum and these modes are confirmed by their TED values. Mostly, the substitutions in the aromatic ring of the title compound affect the ring vibrational modes. In the present study, the bands observed at 1170, 1130, 970 cm^{-1} and 1168 cm^{-1} in the FTIR and Raman spectrum, respectively, have been designated to ring in-plane bending modes by careful consideration of their quantitative descriptions. The ring out-of-plane bending modes of TCNB are also listed in the Table 2. The reductions in the frequencies of these modes are due to the change in force constant and the vibrations of the functional groups present in the molecule. The theoretically computed values for C-C vibrational modes by B3LYP/6-311++G(d,p) method gives excellent agreement with experimental data.

NO_2 vibrations

Aromatic nitro compounds have strong absorptions due to the asymmetric and symmetric stretching vibrations of the NO_2 group at 1570-1485 cm^{-1} and 1370-1320 cm^{-1} region, respectively[16]. Hydrogen bonding has a little effect on the NO_2 asymmetric stretching vibrations[17]. For TCNB, the strong bands at 1602 cm^{-1} in IR and 1595 cm^{-1} in the Raman spectra corresponds to asymmetric stretching modes of nitro group. The symmetric stretching vibration of nitro group is identified at 1360 cm^{-1} in FTIR and 1355 cm^{-1} in the Raman spectrum. The strong band at 750 cm^{-1} in the infrared and the band at 758 cm^{-1} in the Raman spectrum is assigned to NO_2 scissoring mode of TCNB. The deformation vibrations of NO_2 group (rocking, wagging and twisting) contribute to several normal modes in the low frequency region. In the present investigation, the rocking modes of NO_2 group is found at 510 cm^{-1} in both IR and Raman spectra and the NO_2 wagging vibrations of TCNB are observed at 350 cm^{-1} in the Raman spectrum. These assignments are also supported by the literature[17] in addition to TED output.

C-N vibrations

The identification of C-N vibrations is a very difficult task, since mixing of several bands are possible in this region. Silverstein *et al.*[18] assigned C-N stretching absorption in the region 1382-1266 cm^{-1} for aromatic amines. In TCNB, the band observed at 1270 and 1275 cm^{-1} in FTIR and Raman spectra, respectively, are assigned to C-N stretching vibration and the corresponding force constant contribute 81% to the TED. In this study, the bands observed at 630 cm^{-1} in IR is assigned to C-N in-plane bending vibration of TCNB. The slight shift in wavenumber is due to the fact that force constants of the C-N bond increases due to resonance with the ring. The C-N out-of-plane bending vibration has also been identified and is listed in Table 2.

C-Cl vibrations

The vibrations belongs to the bond between the ring and the halogen atoms are worth to discuss here, since mixing of vibrations are possible due to the lowering of the molecular symmetry and the presence of heavy atoms on the periphery of molecule[19]. Generally, the C-Cl absorption is obtained in the broad region[20] between 850 and 550 cm^{-1}. For TCNB, the bands found at 895, 850, 815 cm^{-1} in IR and 890, 820 cm^{-1} in the Raman have been designated to C-Cl stretching mode of vibration and the corresponding force constant contribute nearly 75% to the TED. Most of the aromatic chloro compounds have the band of strong to medium intensity in the region 385-265 cm^{-1} due to C-Cl in-plane bending vibration. Accordingly, in this study, the bands identified at 615, 580 cm^{-1} in FTIR and 612, 575, 400 cm^{-1} in the Raman have been assigned to the C-Cl in-plane mode of TCNB. The C-Cl out-of-plane deformation for TCNB has been established at 260, 205 and 190 cm^{-1} in the Raman spectrum. These are in good agreement with the literature data[20].

Thermodynamic properties

In addition to the vibrational assignments, several thermodynamic parameters are also calculated for the title compound using B3LYP method with 6-31+G(d,p) and 6-311++G(d,p) basis sets and are listed in Table 3. The difference in the values calculated by both the basis sets is only marginal. The global minimum energy obtained for structure optimization of TCNB by DFT/B3LYP with 6-31+G(d,p) and 6-311++G(d,p) basis sets are-1815.52936576 and -1815.71187667 Hartrees, respectively. The specific heat and rotational constants are increasing in values from lower to higher basis sets for B3LYP. The same trends have been observed in entropy calculations. The prediction of accurate dipole moments is very important issue because the magnitude of dipole moment is strongly related to structural stability. If the structural stability is high, dipole moment is lower. In the present study, the total dipole moment of TCNB determined by B3LYP method using 6-31+G (d, p) and 6-311++G(d,p) basis sets is 3.5103 and 3.4734 Debye, respectively.

For the title molecule, the structural stability at B3LYP/6-311++G (d, p) level is high since the dipole moment is lower than one at B3LYP/6-31+G (d, p). The variation in zero-point vibrational energies (ZPVEs) seems to be significant. The total energy and the change in the total entropy of the title compound at room temperature are also presented. According to relationships of thermodynamic functions, one can compute other thermodynamic energies and estimate directions of chemical reactions from the second law of thermodynamics in thermo chemical field.

Table 2: Vibrational assignments of fundamental modes of 1,2,3-trichloro-4-nitrobenzene along with calculated IR intensity (km/mol), Raman activity (Å amu^{-1}) and normal mode descriptions (characterized by TED) based on quantum mechanical calculations using DFT method

Sl. No.	Species C_s	Observed fundamentals (cm^{-1})		Calculated frequencies ν_i (cm^{-1})								TED(%) among types of internal coordinates
				B3LYP/6-31+G(d,p)				B3LYP/6-311++G(d,p)				
		FTIR	Raman	Unscaled ν_i	Scaled	IR intensity	Raman activity	Unscaled ν_i	Scaled	IR intensity	Raman activity	
1	A'	3155(ms)	3150(vw)	3256	3126	10.79	95.80	3234	3105	11.43	96.75	νCH(98)
2	A'	3120(s)	3118(ms)	3232	3102	0.30	80.63	3212	3083	0.47	72.23	νCH(96)
3	A'	1602(ms)	1595(s)	1636	1571	213.09	6.93	1623	1558	206.64	5.26	NO_2 asym(88)
4	A'	1520(vs)	1525(ms)	1606	1542	55.71	83.96	1597	1533	51.65	78.40	νCC(84)
5	A'	-	1494(vw)	1577	1514	62.79	25.54	1568	1505	86.29	27.19	νCC(83)
6	A'	-	1450(vw)	1453	1395	67.02	0.09	1449	1391	71.76	0.04	νCC(80)
7	A'	1422(vs)	-	1385	1329	27.31	0.95	1379	1324	27.45	1.57	νCC(78)
8	A'	-	1435(vw)	1364	1309	334.23	252.63	1350	1296	330.91	222.87	νCC(79)
9	A'	1390(vw)	-	1305	1253	45.08	37.87	1290	1238	42.99	36.45	νCC(81)
10	A'	1360(vs)	1355(vs)	1200	1152	12.84	2.22	1197	1149	12.77	1.98	NO_2 sym(85)
11	A'	1270(s)	1275(ms)	1174	1127	0.57	1.43	1172	1125	0.54	1.21	νCN(81)
12	A'	1190(w)	-	1154	1107	140.72	115.78	1147	1101	147.06	116.58	bCH(78), bCN(18)
13	A'	-	1182(s)	1088	1044	2.94	3.41	1086	1042	3.40	3.81	bCH(79), bCCl(16)
14	A'	1170(s)	1168(w)	984	945	0.30	0.01	983	944	0.42	0.04	R asymd (72), bCH(18)
15	A'	1130(ms)	-	898	862	87.98	2.71	900	864	93.94	2.99	R symd (74), bCN(19)
16	A'	970(w)	-	845	811	23.13	0.42	841	807	26.56	0.21	R trigd (74), bCCl(17)
17	A'	895(vs)	890(ms)	802	770	21.72	1.32	806	774	26.77	1.11	νCCl(74)
18	A'	850(vs)	-	759	728	28.77	3.78	759	729	25.71	3.26	νCCl(73)
19	A'	815(s)	820(w)	747	717	18.52	1.06	719	690	15.85	1.12	νCCl(74)
20	A'	750(s)	758(w)	560	538	14.57	4.08	559	536	13.89	3.92	NO_2 sciss(72)
21	A'	630(w)	-	385	370	1.38	5.87	386	371	1.52	5.82	bCN(71), R asymd (20)
22	A'	615(ms)	612(w)	350	336	0.43	4.68	349	335	0.39	4.42	bCCl(70), R symd (18)
23	A'	580(s)	575(w)	309	297	0.56	2.79	308	296	0.72	2.67	bCCl(69), R trigd (21)
24	A'	510(w)	510(ms)	292	280	1.91	0.39	288	277	1.47	0.21	NO_2 rock (68)
25	A'	-	400(w)	252	242	0.34	0.85	252	242	0.39	0.90	bCCl(70), bCH(18)

26	A"	-	795(w)	686	658	2.22	0.27	639	613	0.58	1.55	ω CH (65), tR asymd (24)
27	A"	780(s)	-	617	593	5.84	4.13	616	591	5.04	3.93	ω CH (66), tR trigd (23)
28	A"	710(ww)	715(w)	556	534	0.45	0.34	542	520	0.61	0.50	tR asymd (64), ω CH (19)
29	A"	695(vw)	-	517	496	0.00	0.32	512	491	0.07	0.46	tR symd (62), ω CN (19)
30	A"	675(vw)	-	507	487	7.19	10.65	505	485	7.24	10.91	tR trigd (63), ω CCl (19)
31	A"	-	350(ms)	248	238	0.46	0.31	244	234	0.35	0.14	NO_2 wagg (62)
32	A"	-	310(s)	220	212	0.13	0.96	221	212	0.13	1.02	ω CN (60), tR asymd (21)
33	A"	-	260(ms)	205	197	0.97	0.95	205	197	0.98	1.02	ω CCl (61), tR asymd (22)
34	A"	-	205(ms)	87	83	2.39	0.63	86	82	2.26	0.63	ω CCl (62), ω CH (19)
35	A"	-	190(ms)	67	64	1.26	0.05	66	63	1.29	0.06	ω CCl (60), ω CN (19)
36	A"	-	150(vw)	56	54	0.04	0.66	62	59	0.06	0.67	NO_2 twist (59)

Abbreviations used: v-stretching; ss – symmetric stretching; ass – asymmetric stretching; b-bending; ω-out-of-plane bending; R-ring; t-torsion; s-strong; vs-very strong; ms-medium strong; w-weak; vw-very weak.

Table 3: The thermodynamic parameters of 1,2,3-trichloro-4-nitrobenzene calculated at the B3LYP/6-311++G(d,p) method.

Parameters	Method/Basis set	
	B3LYP/6-31+G(d,p)	**B3LYP/6-311++G(d,p)**
Optimized global minimum Energy (Hartrees)	-1815.52936576	-1815.71187667
Total energy(thermal), E_{total} (kcal mol^{-1})	52.226	51.933
Heat capacity, C_v (kcal mol^{-1} k^{-1})	0.0352	0.0354
Entropy, S (kcal mol^{-1} k^{-1})		
Total	0.0991	0.0994
Translational	0.0421	0.0421
Rotational	0.0320	0.0320
Vibrational	0.0249	0.0252
Vibrational energy, E_{vib} (kcal mol^{-1})	50.448	50.155
Zero point vibrational energy, (kcal mol^{-1})	46.2077	45.8744
Rotational constants (GHz)		
A	1.0106	1.0140
B	0.4685	0.4693
C	0.3201	0.3208
Dipole moment (Debye)		
μ_x	-1.2725	-1.2862
μ_y	-3.2715	-3.2265
μ_z	0.0000	0.0000
μ_{total}	3.5103	3.4734

Table 4: Second-order perturbation theory analysis of Fock matrix in NBO basis for 1, 2, 3-trichloro-4-nitrobenzene.

Donor (i)	ED (i) (e)	Acceptor (j)	ED (j) (e)	[a]E(2) (kJ mol^{-1})	[b]E(j)–E(i) (a.u.)	[c]F (i,j) (a.u.)
σ(C1 - C2)	0.98875	σ*(C2 - C3)	0.02076	1.97	1.26	0.063
π(C1 - C2)	0.83940	π*(C3 - C4)	0.22814	9.48	0.28	0.067
		π*(C5 - C6)	0.14436	7.73	0.32	0.063
σ(C1 - C6)	0.98769	σ*(C1 - C2)	0.02168	2.00	1.25	0.064
		σ*(C2 -Cl8)	0.01211	2.12	0.89	0.055
σ(C2 - C3)	0.98694	σ*(C1 - C2)	0.02168	2.13	1.27	0.066
		σ*(C1 -Cl7)	0.01334	1.95	0.90	0.053
σ(C3 - C4)	0.98719	σ*(C4 - C5)	0.01001	2.25	1.29	0.068
		σ*(C2 -Cl8)	0.01211	1.94	0.90	0.053
π(C3 - C4)	0.83618	π*(C1 - C2)	0.22263	8.42	0.27	0.062
		π*(C5 - C6)	0.14436	9.41	0.31	0.069
		π*(N10 - O11)	0.30711	9.43	0.17	0.054
σ(C4 - C5)	0.98448	σ*(C3 - C4)	0.01821	2.50	1.24	0.070
		σ*(C3 -Cl9)	0.01171	2.31	0.88	0.057
σ(C5 - C6)	0.98462	σ*(C1 -Cl7)	0.01334	2.29	0.87	0.056
π(C5 - C6)	0.82693	π*(C1 - C2)	0.22263	12.14	0.25	0.071
		π*(C3 - C4)	0.22814	10.43	0.25	0.067
π(N10 - O11)	0.99213	π*(N10 - O11)	0.30711	3.56	0.32	0.051
n3(Cl7)	0.95182	π*(C1 - C2)	0.22263	8.05	0.30	0.068
n3(Cl9)	0.94438	π*(C3 - C4)	0.22814	8.47	0.29	0.069
n2(O11)	0.94828	σ*(C4 - N10)	0.05406	6.85	0.54	0.077
		σ*(N10 - O12)	0.02823	9.55	0.71	0.105
n2(O12)	0.94730	σ*(C4 - N10)	0.05406	6.69	0.54	0.076
		σ*(N10 - O11)	0.02604	8.76	0.72	0.102
n3(O12)	0.73052	π*(N10 - O11)	0.30711	77.84	0.14	0.135
π*(C1 - C2)	0.22263	π*(C5 - C6)	0.14436	37.62	0.04	0.081
π*(C3 - C4)	0.22814	π*(C5 - C6)	0.14436	44.27	0.04	0.083
π*(N10 - O11)	0.30711	π*(C3 - C4)	0.22814	12.01	0.11	0.062
σ*(N10 - O12)	0.02823	σ*(N10 - O11)	0.02604	6.48	0.01	0.051

[a]E(2) means energy of hyper conjugative interactions.

[b]Energy difference between donor and acceptor i and j NBO orbitals.

[c]F(i,j) is the Fock matrix element between i and j NBO orbitals.

HOMO, LUMO analysis

The electronic absorption corresponds to the transition from the ground to the first excited state and is mainly described by one electron excitation from the highest occupied molecular orbital (HOMO) to the lowest unoccupied molecular orbital (LUMO). In TCNB, the LUMO of π nature, (i.e. benzene ring) is delocalized over the whole C-C bond and nitro group. The HOMO is located over the chlorine atoms. Therefore, the HOMO → LUMO transition implies an electron density transfer to C-C bond of the benzene ring and nitro group from chlorine atoms. Moreover, these three orbitals significantly

overlap in the para position of the benzene ring for TCNB. The atomic orbital compositions of the frontier molecular orbital and the HOMO–LUMO energy gap of TCNB was calculated at the B3LYP/6-311++G(d,p) level are shown in Fig. 3. The HOMO-LUMO energy gap for TCNB is found to be 4.571 eV. The LUMO as an electron acceptor represents the ability to obtain an electron, and HOMO represents the ability to donate an electron[21]. Moreover, a lower HOMO–LUMO energy gap explains the fact that ultimate charge transfer interaction is taking place within the molecule which reflects the chemical activity of the molecule.

NBO analysis

Natural Bond Orbital (NBO) analysis is one of the most powerful tools for interpreting quantum-chemical results in terms of chemically significant terms. This study localizes the molecular wave functions in optimized electron pairs, corresponding to lone pairs; core pairs on bonding units; giving a picture which is close to the familiar Lewis picture of molecular structure. In TCNB, the hyperconjugative interaction energy was deduced from the second-order perturbation approach[22]. By the use of the second-order bond–antibond (donor–acceptor) NBO energetic analysis, insight in the most important delocalization schemes was obtained. The change in electron density (ED) of (σ*, π*) antibonding orbitals and E(2) energies have been calculated for TCNB to give clear evidence of stabilization originating from various molecular interactions and are given in Table 4. The electron density of conjugated single as well as double bond of benzene ring (~0.9e) clearly demonstrates strong delocalization for TCNB. The strong intramolecular hyper conjugative interaction of the σ and π electrons of C–C bonding to the C–C antibonding of the ring leads to stabilization of some part of the ring as evident from Table 4. For example, In TCNB, the intramolecular hyper conjugative interaction of σ(C1-C2) → σ*(C2-C3) and π(C1-C2) → π*(C3-C4) leading to stabilization of 1.97 and 9.48 kJ/mol, respectively. The intramolecular interaction are formed by the orbital overlap between bonding and antibonding C-C and C-Cl orbitals which results intramolecular charge transfer (ICT) causing stabilization of the system. These interactions are observed as increase in electron density (ED) in C–C, C–Cl antibonding orbital that weakens the respective bonds. The energies for the interaction n3(Cl7) → π*(C1-C2) and n3(Cl9) → π*(C3-C4) are 8.05 and 8.47 kJmol^{-1}, respectively clearly demonstrate the intramolecular hyper conjugative interaction between the chlorine atoms and benzene ring is strong in the ground state for TCNB . Further, the intermolecular interaction from n3(O12) → π*(N10-O11) leading to the stabilization energy of 77.84 kJmol^{-1}. There occurs a strong intramolecular hyperconjugative interaction of π*(C3-C4)→ π*(C5-C6) which increases electron density that weakens the respective bond (C5-C6 = 1.38 Å) leading to stabilization of 44.27 kJ mol^{-1}. These charge transfer interactions of TCNB are responsible for pharmaceutical and biological properties. Hence the TCNB structure is stabilized by these orbital interactions.

Electrostatic potential, total electron density and molecular electrostatic potential

The electrostatic potential has been used primarily for predicting sites and relative reactivities towards electrophilic attack, and in studies of biological recognition and hydrogen bonding interactions[23]. To predict reactive sites for electrophilic and nucleophilic attack for the investigated molecule, the MEP at the B3LYP/6-311++G(d,p) optimized geometry is calculated. In the present investigation, the electrostatic potential (ESP), electron density (ED) and the molecular electrostatic potential (MEP) map figures for TCNB are shown in Fig. 4. The ED plots for TCNB show a uniform distribution. However, it can be seen from the ESP figures, that the negative ESP is localized more over the nitro group and is reflected as a yellowish blob, the positive ESP is localized on the rest of the molecule. This result is expected, because ESP correlates with electro negativity and partial charges. The negative (red and yellow) regions of the MEP are related to electrophilic reactivity and the positive (blue) regions to nucleophilic reactivity, as shown in Fig. 4. Generally, the potential energy increases from red < orange < yellow < green < blue. In the present study, the MEP map shows that the negative potential sites are oxygen atoms of nitro group (Red) and the positive potential sites are around the nitrogen and hydrogen atoms of the benzene ring (Blue). From these results, one can say that the H atoms indicate the strongest attraction and chlorine atoms indicate the strongest repulsion. These sites provide information about the region of intermolecular interactions for the title compound. Thus, the results indicate that the TCNB will be the most reactive site for both electrophilic and nucleophilic attack.

First hyperpolarizability

The quantum chemistry based prediction of non-linear optical (NLO) properties of a molecule has an essential role for the design of materials in modern communication technology, signal processing and optical interconnections[24,25]. Especially organic molecules are studied because of their larger NLO susceptibilities arising π-electron cloud movement from donor to acceptor, fast NLO response times, high laser damage thresholds and low dielectric constants. The total static dipole moment μ, the average linear polarizability $\overline{\alpha}$, the anisotropy of the polarizability Δα, and the first hyperpolarizability β can be calculated by using the following equations[25]:

The calculated values of total static dipole moment μ, the average linear polarizability $\overline{\alpha}$, the anisotropy of the polarizability Δα, and the first hyperpolarizability β using the DFT-B3LYP/6-311++G(d,p) method are 3.4734 Debye, 18.61 Å^3, 14.01 Å^3 and 8.495×10^{-30} e.s.u.$^{-1}$, respectively. The values of μ, $\overline{\alpha}$ and β obtained by Sun *et al.*[26] with the B3LYP method for urea are 1.373 Debye, 3.831 Å^3 and

0.3729×10^{-30} e.s.u.$^{-1}$, respectively. The first hyperpolarizability of TCNB molecule is 23 times greater than that of urea. According to these results, the title compound may be a potential candidate for the development of NLO materials.

$$\overline{\alpha} = \frac{1}{3}(\alpha_{xx} + \alpha_{yy} + \alpha_{zz})$$

$$\Delta\alpha = \frac{1}{\sqrt{2}}\left[[(\alpha_{xx} - \alpha_{yy})^2 + (\alpha_{yy} - \alpha_{zz})^2 + (\alpha_{zz} - \alpha_{xx})^2 + 6\alpha_{xx}^2]\right]^{1/2}$$

$$\mu = (\mu_x^2 + \mu_y^2 + \mu_z^2)^{1/2}$$

$$\beta = [(\beta_{xxx} + \beta_{xyy} + \beta_{xzz})^2 + (\beta_{yyy} + \beta_{xxy} + \beta_{yzz})^2 + (\beta_{zzz} + \beta_{xxz} + \beta_{yyz})^2]^{1/2}$$

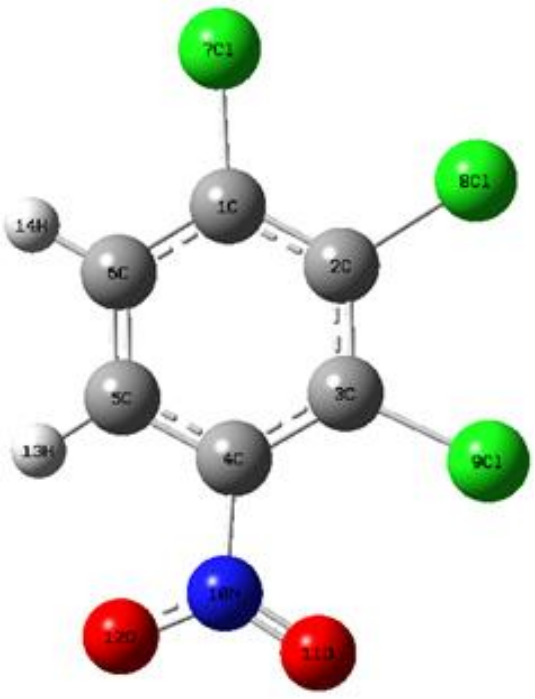

Figure 1: Molecular structure of 1, 2, 3-trichloro-4-nitrobenzene.

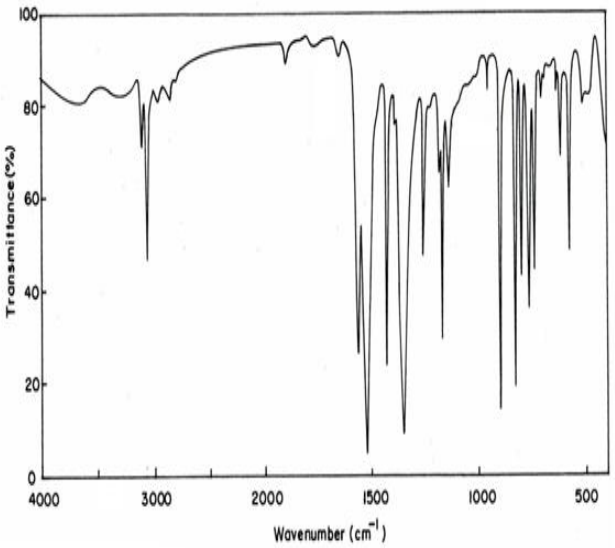

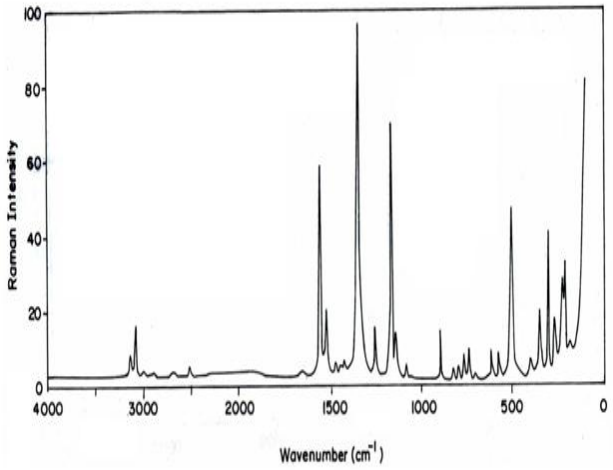

Figure 2: FTIR and FT-Raman spectra of 1, 2, 3-trichloro-4-nitrobenzene.

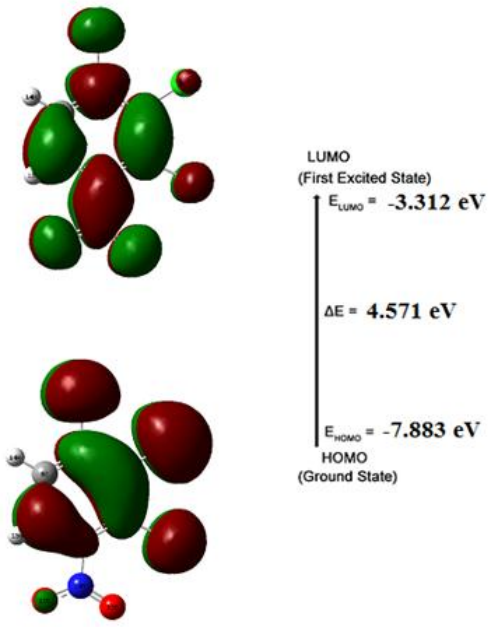

Figure 3: Frontier molecular orbital for 1,2,3-trichloro-4-nitrobenzene.

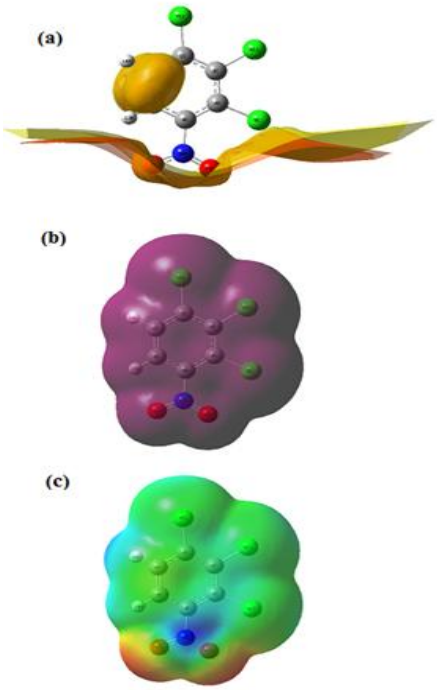

Figure 4: (a) Electrostatic potential (ESP); (b) electron density (ED) and (c) the molecular electrostatic potential (MEP) map for 1, 2, 3-trichloro-4-nitrobenzene.

CONCLUSION

Based on the SQM force field obtained by DFT/B3LYP method with 6-31+G(d,p) and 6-311++G(d,p) basis sets, a complete vibrational properties of 1,2,3-trichloro-4-nitrobenzene have been investigated by FTIR and FT-Raman spectroscopies. The various modes of vibrations were unambiguously assigned based on the results of the TED output. The HOMO and LUMO energy gap explains the eventual charge transfer interactions taking place within the molecule. NBO results reflect the charge transfer mainly due to the lone pair n3(O12) → π*(N10-O11), n3(Cl7) → π*(C1-C2) and n3(Cl9) → π*(C3-C4) interactions. The MEP map shows the negative potential sites are on oxygen atom as well as the positive potential sites are around the hydrogen atoms. Furthermore, the polarizability, the first hyperpolarizability and total dipole moment of title molecule have been calculated and the results are discussed. These results indicate that the TCNB compound is a good candidate of nonlinear optical materials.

REFERENCES

1. Goto Y, Hyashi A, Kimura Y, Nakayama SM, Second harmonic generation and crystal growth of substituted thienyl chalcone, J. Cryst. Growth. 108, 1991, 688-698.
2. Arjunans V, Mohan S, Fourier transform infrared and FT-Raman spectral analysis and ab initio calculations for 4-chloro-2-methylaniline and 4-chloro-3-methylaniline, J. Mol. Struct., 892, 2008, 289-299.
3. Mahadevan D, Periandy S, Karabacak M, Ramalingam S, FT-IR and FT-Raman, UV spectroscopic investigation of 1-bromo-3-fluorobenzene using DFT (B3LYP, B3PW91 and MPW91PW91) calculations, Spectrochim. Acta, 82A, 2011, 481-492.
4. Kolesnikova IN, Dorofeeva OV, Karasev NM, Oberhammer H, Shishkov IF, Molecular structure and conformation of 1,3,5-tris(trifluoromethyl)-benzene as studied by gas-phase electron diffraction and quantum chemical calculations, J. Mol. Struct., 1074, 2014, 196–200.
5. Hosseinzadeh R, Moosavi-Movahedi AA, Human hemoglobin structural and functional alterations and heme degradation upon interaction with benzene: A spectroscopic study, Spectrochim. Acta, 157A, 2016, 41–49.
6. Vennila P, Govindaraju M, Venkatesh G, Kamal C, Armaković SJ, A complete computational and spectroscopic study of 2-bromo-1, 4-dichlorobenzene – A frequently used benzene derivative, J. Mol. Struct., 1151 (2018) 245– 255.
7. Becke AD, Density-functional thermochemistry. III. The role of exact exchange, J. Chem. Phys. 98, 1993, 5648–5652.
8. Lee C, Yang W, Parr RR, Development of the Colle-Salvetti correlation-energy formula into a functional of the electron density, Phys. Rev. B 37, 1988, 785–789.
9. Frisch MJ, Trucks GW, Schlegel HB, Scuseria GE, Robb MA, Cheeseman JR, Scalmani G, Barone V, Mennucci B, Petersson GA, Nakatsuji H, Caricato M, Li X, Hratchian HP, Izmaylov AF, Bloino J, Zheng G, Sonnenberg JL, Hada M, Ehara M, Toyota K, Fukuda R, Hasegawa J, Ishida M, Nakajima T, Honda Y, Kitao O, Nakai H, Vreven T, Montgomery JA, Peralta JE, Ogliaro F, Bearpark M, Heyd JJ, Brothers E, Kudin KN, Staroverov VN, Kobayashi R, Normand J, Raghavachari K, Rendell A, Burant JC, Iyengar SS, Tomasi J, Cossi M, Rega N, Millam JM, Klene M, Knox JE, Cross JB, Bakken V, Adamo C, Jaramillo J, Gomperts R, Stratmann RE, Yazyev O, Austin AJ, Cammi R, Pomelli C, Ochterski JW, Martin RL, Morokuma K, Zakrzewski VG, Voth GA, Salvador P, Dannenberg JJ, Dapprich S, Daniels AD, Farkas O, Foresman JB, Ortiz JV, Cioslowski J, Fox DJ, GAUSSIAN 09, Revision A.02, Gaussian Inc, Wallingford CT, 2009.
10. MOLVIB (V.7.0): Calculation of Harmonic Force Fields and Vibrational Modes of Molecules, QCPE Program No. 807, 2002.
11. Hazell RG, Lehmann MS, Pawley GS, The Crystal Structure of 1,2,3-trichlorobenzene; Neutron Diffraction and Donstrained Refinements, Acta Cryst., B28, 1972, 1388–1394.
12. Barnett SA, Johnston A, Florence AJ, Kennedy AR, 3,4-Dichloro-1-nitrobenzene–1,4-dioxane (4/1), Acta Cryst., E61, 2005, o3666–o3667.
13. Young DC, Computational Chemistry: A Practical Guide for Applying Techniques to Real World Problems (Electronic), John Wiley & Sons Ltd., New York, 2001.
14. Gobinath E, Jeyavijayan S, John Xavier R, Spectroscopic investigations, DFT computations and other molecular properties of 2,4dimethylbenzoicacid, Indian J. Pure & Appl. Phys., 55, 2017, 541-550.
15. Jeyavijayan S, Molecular structure, vibrational spectra, NBO analysis, first hyperpolarizability, and HOMO–LUMO studies of 2-amino-4- hydroxypyrimidine by density functional method, J. Mol. Struct., 1085, 2015, 137–146.

16. Kavitha E, Sundaraganesan N, Sebastian S, Molecular structure, vibrational spectroscopic and HOMO, LUMO studies of 4-nitroaniline by density functional method, Indian J. Pure Appl. Phys., 48, 2010, 20-30.

17. Sathyanarayana DN, Vibrational Spectroscopy - Theory and Applications, Second ed., New Age International (P) Limited Publishers, New Delhi, 2004.

18. Silverstein M, Basseler GC, Morill C, Spectrometric Identification of Organic Compounds, Wiley, New York, 1981.

19. Doly M. Chemes DM, Alonso de Armiño DJ, Cutin EH, Oberhammer H, Robles NL, Synthesis, characterization and vibrational studies of p-chlorosulfinylaniline, J. Mol. Struct., 1127, 2017, 191-198.

20. Arjunan V, Mohan S, Fourier transform infrared and FT-Raman spectral analysis and ab initio calculations for 4-chloro-2-methylaniline and 4-chloro-3-methylaniline, J. Mol. Struct., 892, 2008, 289-299.

21. Jeyavijayan S, Spectroscopic (FTIR, FT-Raman), molecular electrostatic potential, NBO and HOMO–LUMO analysis of P-bromobenzene sulfonyl chloride based on DFT calculations, Spectrochim. Acta, 136A, 2015, 890–899.

22. Singh P, Islam SS, Ahmad H, Prabaharan A, Spectroscopic investigation (FT-IR, FT-Raman), HOMO-LUMO, NBO, and molecular docking analysis of N-ethyl-N-nitrosourea, a potential anticancer agent, J. Mol. Struct., 1154, 2018, 39-50.

23. Murray JS, Sen K, Molecular Electrostatic Potentials, Concepts and Applications, Elsevier, Amsterdam, 1996, pp. 7–624.

24. Geskin VM, Lambert C, Bredas JL, Origin of high second-and third-order nonlinear optical response in ammonio/borato diphenylpolyene zwitterions: the remarkable role of polarized aromatic groups, J. Am. Chem. Soc. 125, 2003, 15651-15658.

25. Sajan D, Hubert Joe I, Jayakumar VS, Zaleski J, Structural and electronic contributions to hyperpolarizability in methyl p-hydroxy benzoate, J. Mol. Struct., 785, 2006, 43-53.

26. Sun YX, Hao QL, Wei WX, Yu ZX, Lu LD, Wang X, Wang YS, Experimental and density functional studies on 4-(3,4-dihydroxybenzylideneamino)antipyrine, and 4-(2,3,4-trihydroxybenzylideneamino)antipyrine, J. Mol. Struct. (Theochem.) 904, 2009, 74-82.

Source of Support: Nil, **Conflict of Interest:** None.